

# Chapter 2

## Experimental Methodology

### 2.1 Particle Accelerators and Applications

After the discovery of the atomic nucleus by scattering  $\alpha$ -particles off gold foil by Rutherford in 1911, the development of high energy accelerators began. Since then, high voltage DC and RF accelerators have been developed and high-field magnets with excellent field quality have been achieved. Accelerator science took off in the 20<sup>th</sup> century and became evolving branch of science. Many innovative technologies invented to produce and manipulate high energy and high quality beams in accelerator science which will help to study natural and biomedical science. In 21<sup>st</sup> century, accelerators will have a key role in the application of industrial processing and imaging, biomedical research, nuclear medicine, medical imaging, cancer therapy, energy research etc. [1-2].

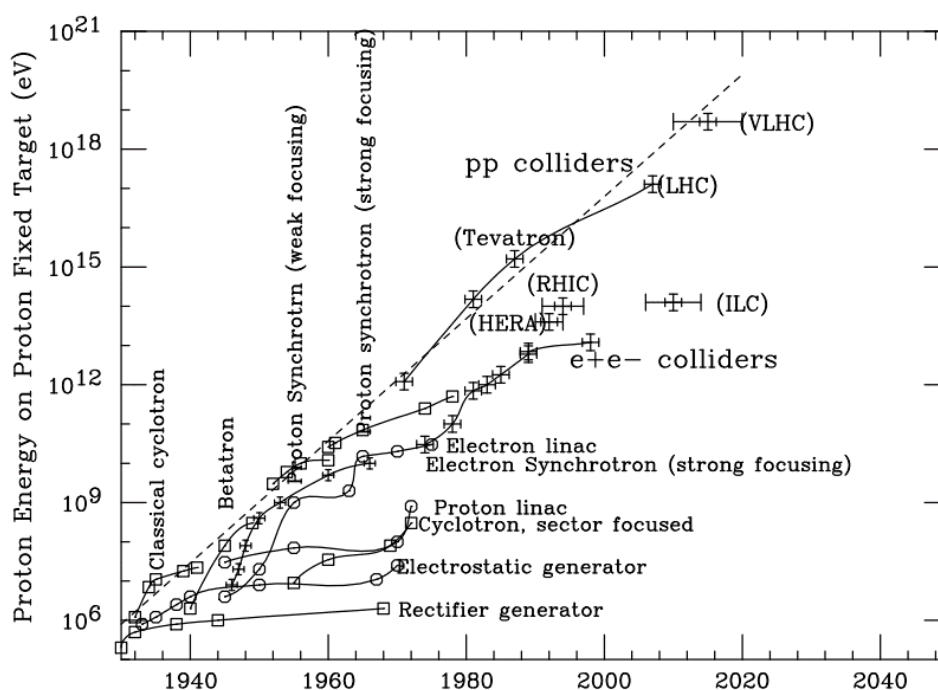


Figure 2.1 The Livingston chart of fixed target proton beam energy versus time in years [3]

A major application of particle accelerators is experimental nuclear and particle physics. The evolution of development of accelerators is shown in Figure 2.1 by the Livingston chart where the proton kinetic energy for a fixed target experiment is plotted as a function of time. In the

last decades the accelerator development has been impressive. As seen in *Figure 2.1*, high energy was measured in MeV's in 1930's, GeV's in the 1950's and multi-TeV's run in the 1990's. In the coming decades, the center of mass energy will reach 10-100 TeV. Advancement in high power accelerator technologies have applications in material science and medical research with spallation neutron sources, studies of the interaction between the charged particles and electromagnetic field, nuclear transmutation of the nuclear wastes, energy production and national security. In all over the world various activities are going on by scientists to build a modern advanced accelerator for various applications. Accelerators can be classified as linear or circular, electrostatic or radio frequency, continuous or pulsed. They are designed to accelerate electrons, stable or radioactive ions. Accelerators have been classified as natural accelerators, electrostatic accelerators, induction accelerators, radio-frequency (RF) accelerators and colliders and storage rings. In the application of nuclear techniques, various types of neutron sources are available over a long history which are summarized in the next section.

## 2.2 Neutron Sources

---

The term neutron source refers to any device that emits neutrons, regardless of the mechanism behind its production. In 1970s, proton accelerators were constructed to access neutrons via spallation, which gave rise to the production of neutrons by accelerators. Meanwhile, electron accelerators, ion beam accelerators, cyclotrons, and linear accelerators with low energy became viable for producing neutrons. The neutrons are also produced in the fission-fusion reactors and high-energy particle accelerators like Accelerator Driven System (ADS). The major neutron sources available for research purpose are the research fission reactors. ARGONAUT, HOMOG(S), POOL, TANK, TANK in POOL, and TRIGA are the types of fission reactors, in which reactor fuel is made of U-Al alloy,  $\text{UO}_2$  in polyethylene,  $\text{U}_3\text{Si}_2\text{Al}_x$ ,  $\text{UO}_2$  and  $\text{UAl}_x$  [4, 5]. Generally, research reactors have a small core sizes because neutron flux is a function of neutron density and also it is proportional to the power of the system. The average neutron flux of a research reactor is in a range of  $10^6$  to  $10^{15}$  n/cm<sup>2</sup>s. Another type of neutron source is a spallation neutron source which is an accelerator based pulsed neutron source. A spallation is a process in which a proton of energy hundreds of MeV or GeV knock out some neutrons from a heavy atomic nucleus like mercury, lead, tungsten and uranium. Further additional neutrons are emitted as a heavy atomic nucleus left in its excited states. Therefore, compared to fission reactors, spallation neutron sources produce more neutrons per unit energy in the system [6, 7].

The neutrons are produced by the interaction of charged particles. Some of the reactions are  ${}^3\text{H}(p,n){}^3\text{He}$ ,  ${}^7\text{Li}(p,n){}^7\text{Be}$ ,  ${}^9\text{Be}(p,n){}^9\text{B}$ , and  ${}^9\text{Be}(d,n){}^{10}\text{B}$ . The list of the reactions with neutron energy is given in *Table 2.1* [8-10]. Although the neutron yields of these reactions are not as high as the spallation process, these reactions have their own applications. To get a reasonable neutron yield, high energy (>MeV) accelerator are required.

*Table 2.1 List of reactions produces neutrons of different energies*

<i>Reaction</i>	<i>Q-Value (MeV)</i>	<i>Threshold (MeV)</i>	<i>Neutron Energy (MeV)</i>
<i>Charged Particle</i>			
${}^3\text{H}(p,n){}^3\text{He}$	-0.763	1.018	0.3-7.6
${}^7\text{Li}(p,n){}^7\text{Be}$	-1.644	1.880	
${}^9\text{Be}(p,n){}^9\text{B}$	-1.852	2.057	
${}^9\text{Be}(d,n){}^{10}\text{B}$	4.36	-	
<i>Radioisotope Source</i>			
${}^{252}\text{Cf}$	-	-	2.0
<i>AmBe</i>	-	-	4.2
<i>Fusion</i>			
<i>D-D</i>	3.268	-	2.5
<i>T-T</i>	11.33	-	0-9
<i>D-T</i>	17.58	-	14.1

There are some isotopes which emits neutrons by spontaneous fission process. The most common isotope is californium-252 ( ${}^{252}\text{Cf}$ ) which have a fission neutron spectrum. This type of sources are prepared by irradiation of uranium and transuranic elements type target materials

in a reactor. The neutrons are absorbed by the target materials which converts in to spontaneous fission isotopes by the transmutation process. Generally the neutron yield from the  $^{252}\text{Cf}$  neutron source is  $10^7$  to  $10^9$  n/s which drops down by half in 2.6 years. Another type of radioisotope neutron source is made by mixing an alpha emitter e.g. radium, polonium and/or americium with a low atomic weight isotope having high ( $\alpha$ , n) reaction cross section. These sources produced  $10^6$  to  $10^8$  neutrons per second. In contrast to radioactive isotopes, there are various types of neutron sources, including deuterium (D, hydrogen-2) and tritium (T, hydrogen-3) fusion reactions which are mentioned in *Table 2.1*. The neutrons are produced by accelerating ions of deuterium, tritium or deuterium and tritium into a hydride target loaded with deuterium or tritium. Since the neutron yield of the D T reaction is 50-100 times higher than the D D reaction, therefore D T reaction is used more than the DD- reaction.

## 2.3 Neutron Irradiation Facility

---

As discussed in the previous section, the neutrons are produced by different techniques but the most common method to produce high intense neutrons is by using the accelerator system. The following are the charged particle interaction based neutron facilities that are employed in the current research project for the experiments.

### 2.3.1 Folded Tandem Ion Accelerator (FOTIA)

---

A 6 MV Folded Tandem Ion Accelerator (FOTIA) facility was commissioned in 2000 at Nuclear Physics Division in BARC, Mumbai-India [11-13]. In this accelerator, the extracted negative ions from a SNICS-II ion source at 150 keV are inserted into a low energy accelerating tube with the help of  $70^\circ$  magnet and  $20^\circ$  electrostatic deflector. When the negative ions pass through the foil stripper, they become positive ions after being accelerated to the positive high voltage (up to 6 MV) terminal. Through the  $180^\circ$  folding magnet, positive ions of a particular charge state are bent and then again accelerated to a ground potential through the high energy accelerating tube. The beam is guided to the scattering chamber for experimental purposes after being analysed by the  $90^\circ$  bending magnet. A schematic diagram of the FOTIA accelerator is presented in *Figure 2.2* with experimental facility. The quasi mono-energetic neutrons in the energy range 0.6 - 3.2 MeV are produced by hitting proton beam of energies 2 - 5 MeV to the natural lithium (Li) target via  $^7\text{Li}(p,n)^7\text{Be}$  charged particle reaction. The detailed discussion for experiments carried out using FOTIA facility is presented in Chapter 4.

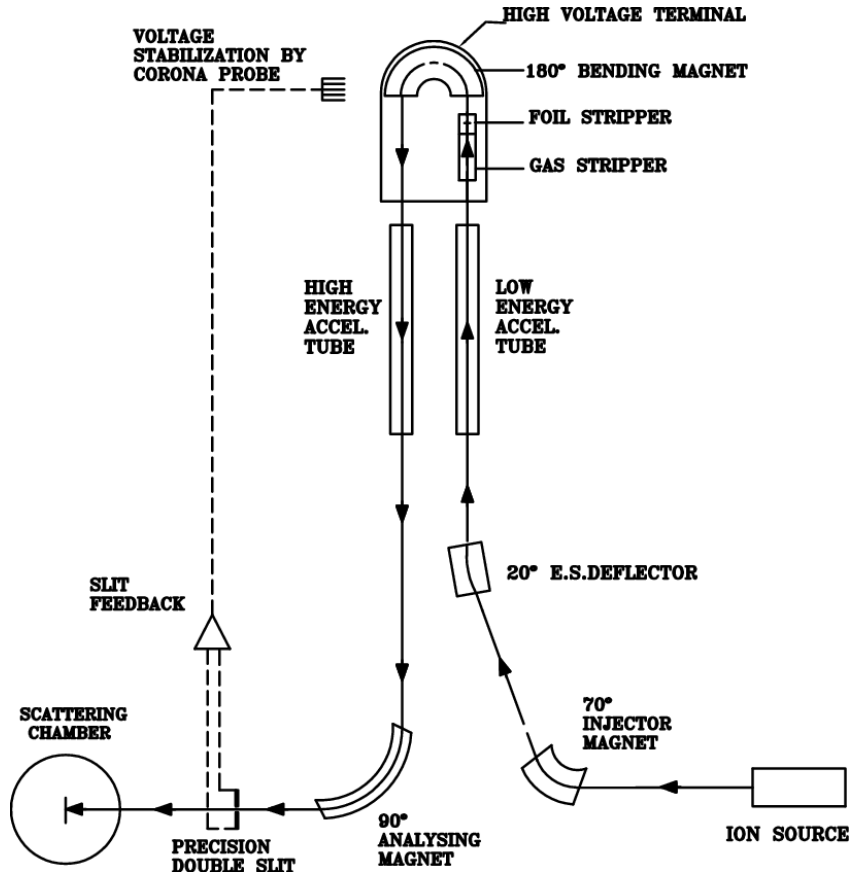


Figure 2.2 Schematic diagram of 6 MV FOTIA at BARC facility [12]

### 2.3.2 14UD Pelletron Accelerator

The 14UD Pelletron-Linac facility is a joint set up between Nuclear Physics Division (NPD), BARC and TIFR, Mumbai-India, commissioned in 1988 [14, 15]. Since then it has been in operation and utilized for the heavy ion accelerator based research and applications. In TIFR-BARC Pelletron facility, using 12 MV as the terminal voltage, it is possible to generate proton beam of energy of 22 MeV. As mentioned above in FOTIA facility, the neutron beam was generated from  ${}^7\text{Li}(p,n)$  and  ${}^9\text{Be}(p,n)$  reaction using proton beam in 6 meter main beam line above the analyzing magnet. With these reactions, a neutron yields up to  $10^7 - 10^8$  n/s was achieved using few MeV protons and hundreds of nano-ampere (nA) beam current. To regulate the terminal voltage, a terminal potential stabilizer was used by generating voltage mode. A schematic diagram of TIFR-BARC Pelletron facility is shown in *Figure 2.3* along with neutron production set up. The experiments are performed using TIFR-BARC Pelletron facility for 8 - 22 MeV proton beam energies was discussed in next chapter 5.

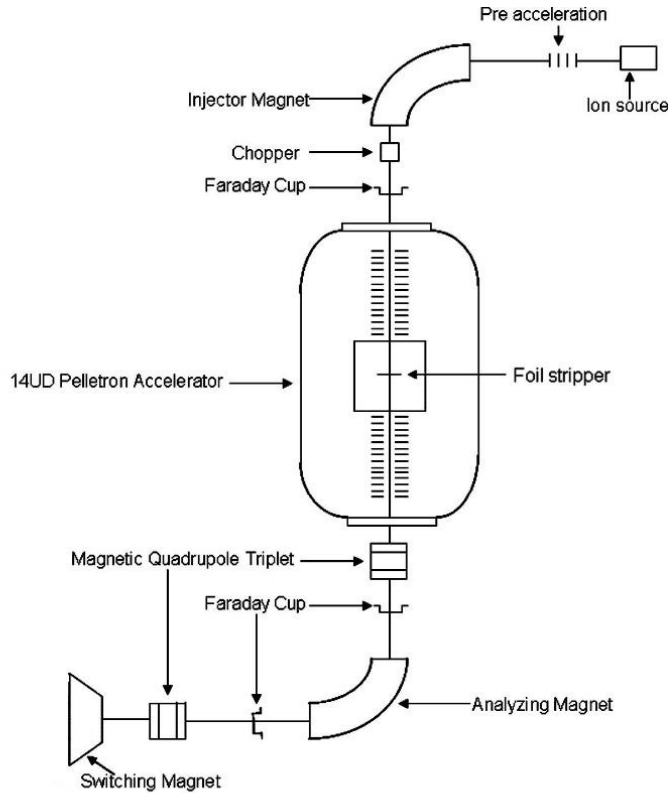


Figure 2.3 Schematic diagram of 14UD Pelletron Accelerator at TIFR-BARC facility [14]

## 2.4 Activation Analysis

As discussed in Chapter -1, the reaction cross section is determined by the technique called Neutron Activation Analysis [16]. This technique is commonly employed for both qualitative and quantitative analysis of elements. It involves measuring the characteristic radiation emitted from the target nucleus after it has been activated by neutron irradiation. Research reactors are typically used as the neutron sources for such applications. *Figure 2.4* illustrates the neutron activation process through a schematic diagram. The target nucleus is bombarded with neutrons to form a compound nucleus which equilibrated via emission of prompt  $\gamma$ -rays or n, p,  $\alpha$ -particles [17]. After equilibrium is achieved, the compound nucleus decays into a radionuclide by emitting delayed  $\gamma$ -rays and  $\beta$ -particles. The emitted  $\gamma$ -rays are recorded by the detector from which the suitable information can be extracted for the cross section measurements.

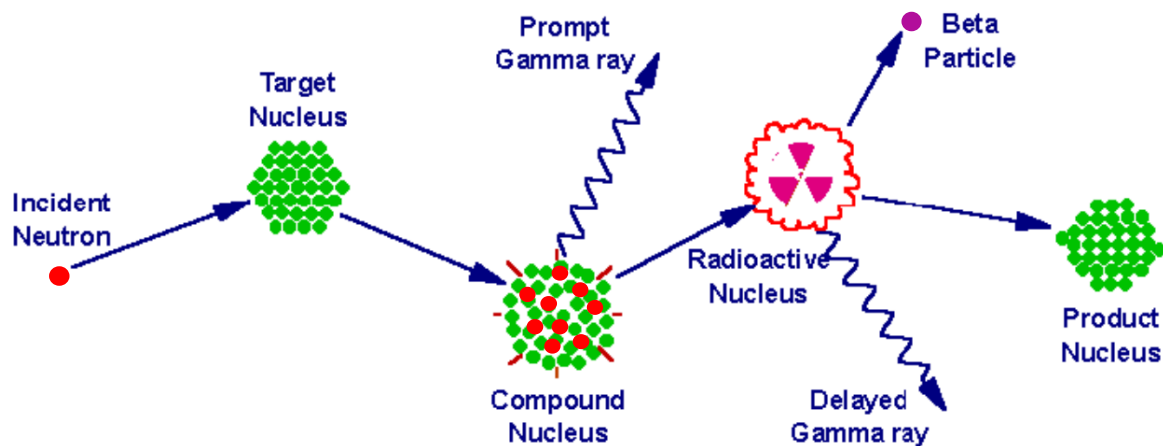


Figure 2.4 Schematic representation of Neutron Activation Analysis Technique (NAA) [16]

### 2.4.1 $\gamma$ -ray Spectroscopy

In neutron irradiation experiments, the induced activity in the target sample is measured by the  $\gamma$ -ray spectroscopy method. [18, 19] In this method, the activity is measured by two techniques: (i) **Online  $\gamma$ -ray spectroscopy**: in which during irradiation, prompt  $\gamma$ -rays or particles produced from compound nucleus are recorded by the detector; (ii) **Offline  $\gamma$ -ray spectroscopy**: in which after irradiation is over, the delayed  $\gamma$ -rays produced after formation of compound nucleus is recorded by the detector. In this work, the  $\gamma$ -ray spectrum is recorded by a pre-calibrated HPGe detector offline. The advantage of offline spectroscopy is one can record the  $\gamma$ -ray spectrum repetitively for different samples and record  $\gamma$ -ray spectrum over an extensive time for longer half-life isotopes. In the  $\gamma$ -ray spectroscopy method, the most important thing is selection of suitable HPGe detector for our applications. The complete discussion about the HPGe detector is given as follows.

### 2.4.2 High Purity Germanium (HPGe) detector

A semiconductor detector used for  $\gamma$ -ray spectroscopy, known as an HPGe detector, is made from ultrafine germanium. As shown in Figure 2.5, the detector design is coaxial to absorb the maximum number of  $\gamma$ -rays. Both the inside and outside of the coaxial are connected to the electrodes. Electron-hole pairs are generated when a charged particle interacts with the

detector. A potential is applied across the coaxial and the detector due to this electron-hole pairs have to travel in different distance. Therefore the collection time of these pairs to reach the electrodes are different which results in different pulse shape in the recorded spectrum.

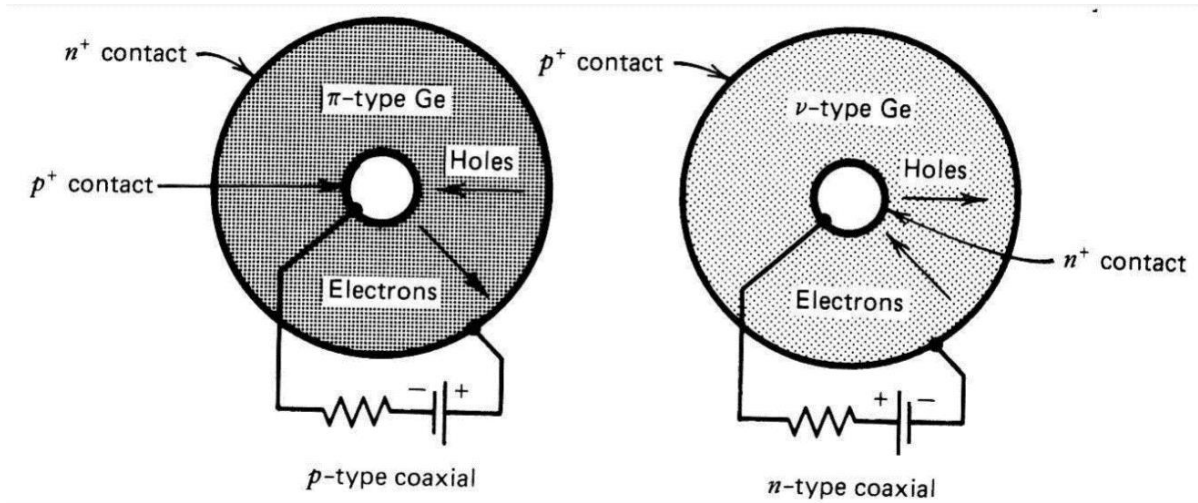


Figure 2.5 Cross section of the detector crystal perpendicular to the cylindrical axis [18]

HPGe detectors are not operated at room temperature due to the small bandgap ( $\sim 0.7$  eV), leakage current induced at room temperature. This leakage current will spoil the energy detection. Therefore the germanium detector is housed in a vacuum tight cryostat cooled with liquid nitrogen to achieve the great energy resolution. A schematic sketch of such device is presented in Figure 2.6.

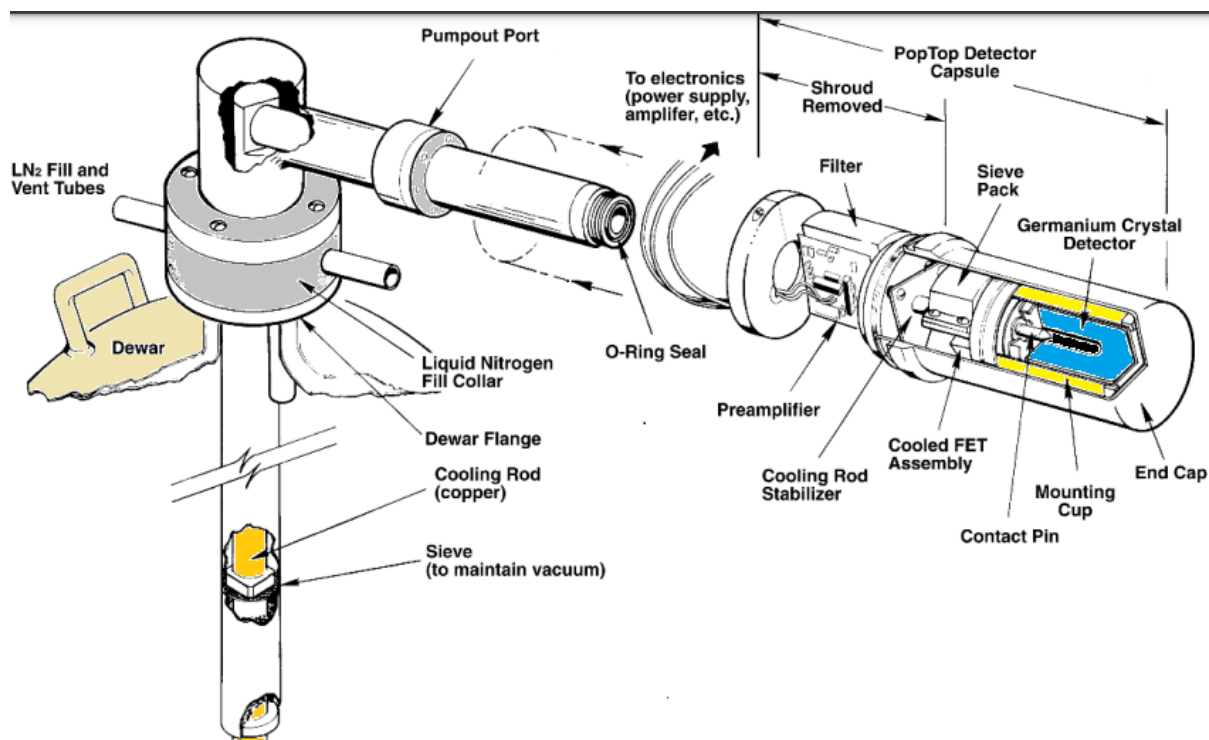


Figure 2.6 Schematic diagram of HPGe detector [19]

### 2.4.3 Energy resolution

In  $\gamma$ -ray spectroscopy, excellent energy resolution is achieved by the germanium detectors which means the detector is able to discriminate the difference between the  $\gamma$ -rays of similar energies. A high resolution detector has more defined  $\gamma$ -ray spectrum. In present work, each HPGe detector is calibrated with  $^{152}\text{Eu}$  standard  $\gamma$ -ray source with known activity. Table 2.2 contains the details of each  $^{152}\text{Eu}$ -source utilized in this work. The source has prominent  $\gamma$ -energies ranging from 0.122 MeV to 1.408 MeV. The  $\gamma$ -ray energies used for the calibration of HPGe detector are presented in Table 2.3.

Table 2.2 Details of  $^{152}\text{Eu}$ -source

Facility	Source	Activity (Bq)	Manufacture date	Half-life
FOTIA	$^{152}\text{Eu}$ - standard	$6659.2 \pm 82$	1-October-1999	13.517 (9) year
TIFR-BARC	source	$7767.73 \pm 88.1$	1-October-1999	

Table 2.3 Characteristic  $\gamma$  -ray energies of  $^{152}\text{Eu}$ -source [10]

$E_\gamma$ (keV)	$I_\gamma$
121.78	$0.2853 \pm 0.0016$
244.69	$0.0755 \pm 0.0004$
344.27	$0.2659 \pm 0.0020$
443.96	$0.02827 \pm 0.00014$
778.90	$0.1293 \pm 0.0008$
964.05	$0.1451 \pm 0.0007$
1085.83	$0.1011 \pm 0.0005$
1112.07	$0.1367 \pm 0.0008$
1408.01	$0.2087 \pm 0.0009$

The excellent resolution of the germanium detector is due to: the inherent statistical spread in the quantity of charge carriers, discrepancies in the efficiency of charge collection, and the impact of electronic interference. Some of these factors will dominate over the other factors, but this is dependent on the energy of the radiation and the size and quality of the detector in use.

#### 2.4.4 Efficiency calibration

The efficiency of the HPGe detector is determined by employing a standard  $^{152}\text{Eu}$  source. A typical  $\gamma$ -ray spectrum recorded by detector is presented in *Figure 2.7* with the  $\gamma$ -ray energies listed in *Table 2.3*. The detector efficiency is determined by the following equation:

$$\varepsilon = \frac{C K_C}{A_0 I_\gamma \exp^{-\lambda T \Delta t}} \quad (2.1)$$

Where,  $C$  is the counts for a interested  $\gamma$ -ray line in the time interval  $\Delta t$  with the absolute intensity ( $I_\gamma$ ),  $A_0$  is the activity of  $^{152}\text{Eu}$  source at manufacturing time,  $\lambda$  is the decay constant and  $T$  is the time interval between the manufacturing date and counting date.  $K_C$  is the summing correction factor determined using the EFTRAN code [20]. The efficiency with fitted curve is presented in *Figure 2.8*.

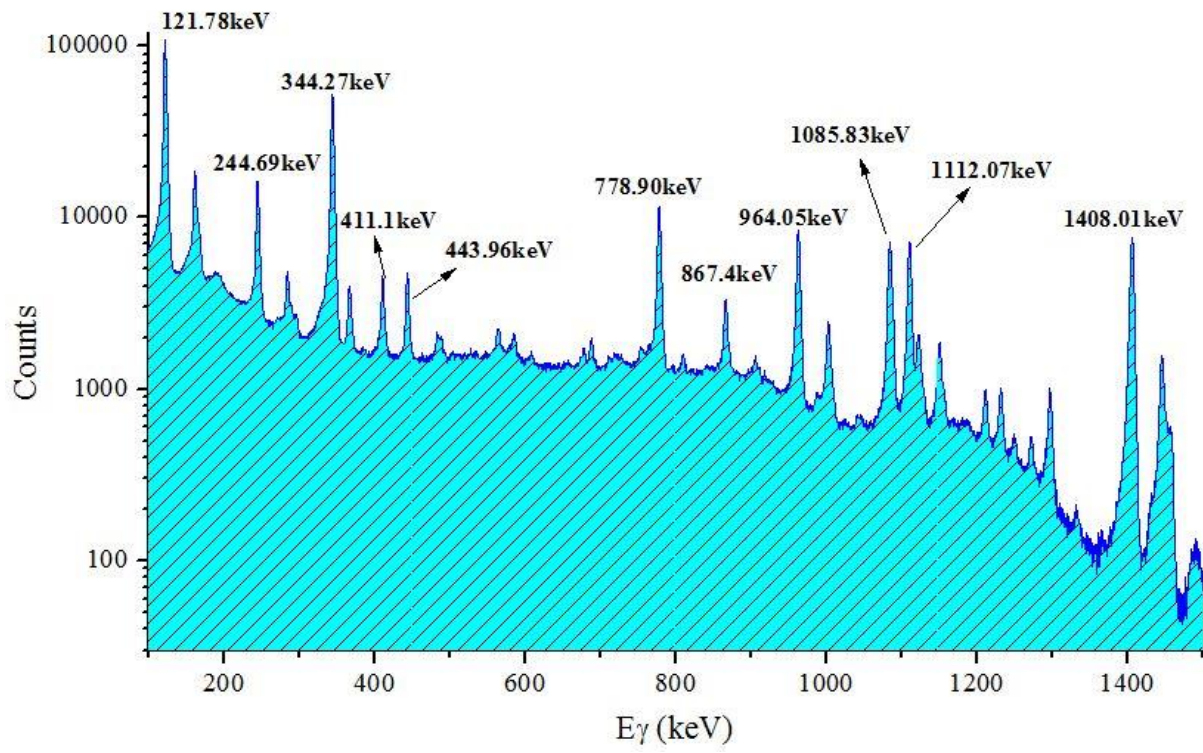


Figure 2.7 A typical  $\gamma$ -ray spectrum of  $^{152}\text{Eu}$  source

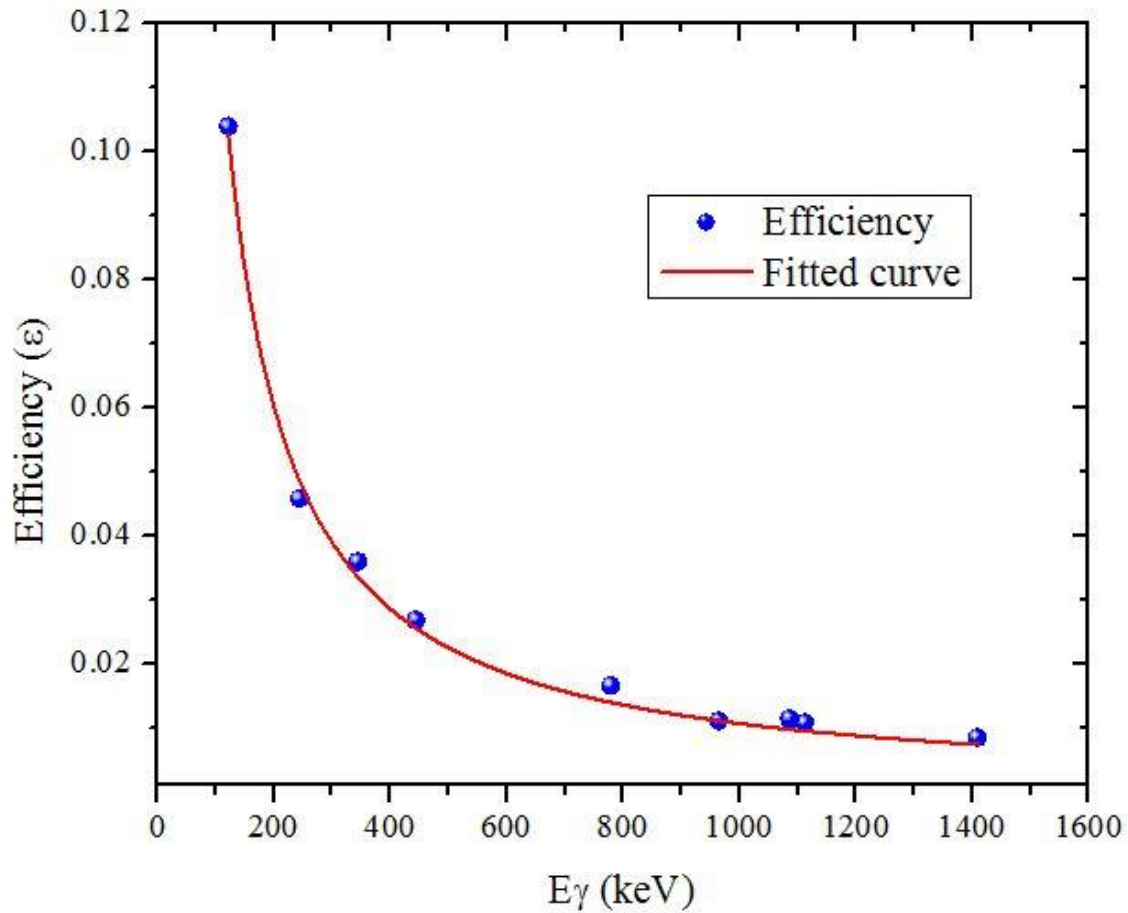


Figure 2.8 Measured efficiency and fitted curve for  $^{152}\text{Eu}$  source

### 2.4.5 Background radiation

In the  $\gamma$ -ray spectroscopy, the background spectrum is also important to analyze. The recorded  $\gamma$ -ray spectrum by detector consist the background radiation from the natural activity of the constituent materials of the detector, the natural radioactivity from the surrounding materials of the detector and also from the cosmic radiations. The prominent sources for background radiations are  $^{232}\text{Th}$ ,  $^{238}\text{U}$ ,  $^{235}\text{U}$ , and  $^{40}\text{K}$  and their daughter nuclides. The background correction in the recorded  $\gamma$ -ray spectrum is needed to avoid false measurements for a source that is being measured. *Figure 2.9* represents the recorded spectrum having  $\gamma$ -ray energies in the detector background and the environment.

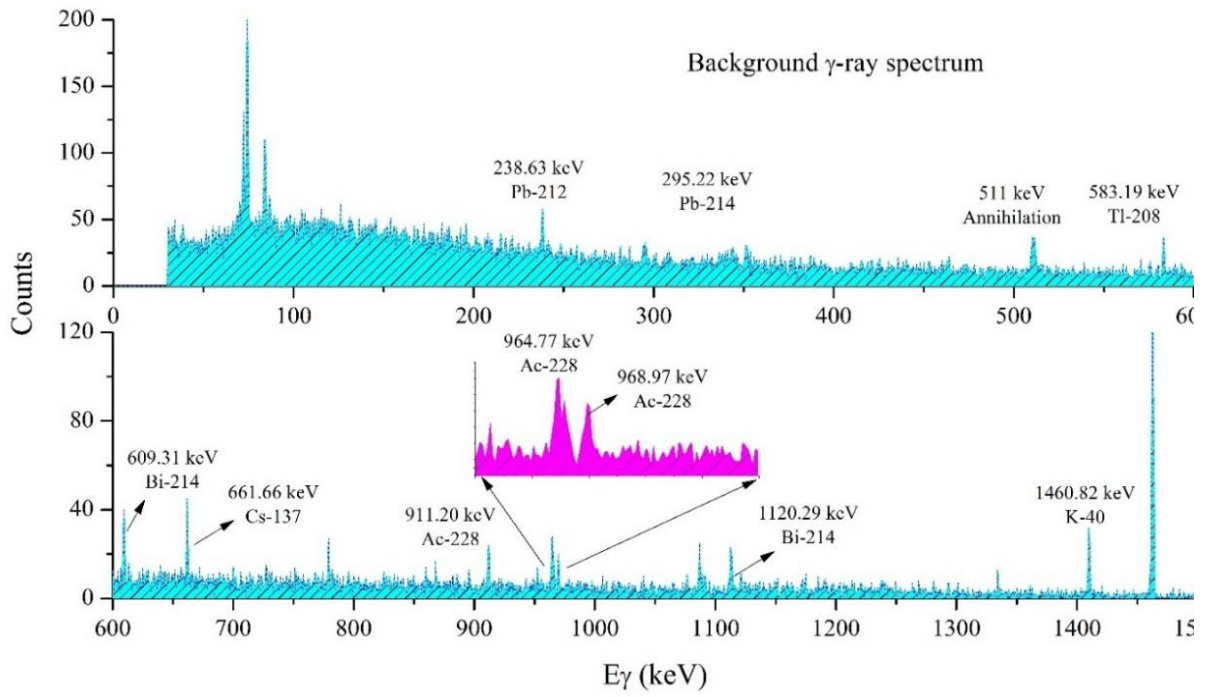


Figure 2.9 Background spectrum recorded by HPGe detector for  $t=600$  sec

## References

---

- [1]. O. Barbalat, Applications of particle accelerators, In S. Turner (Ed.). CAS CERN accelerator school: 5 general accelerator physics course Vol. 2 proceedings, (pp. 537) European Organization for Nuclear Research (CERN), 1994.
- [2]. J. D. Lawson, Nuclear Instruments and Methods in Physics, 220 (1) (1984) 217-223.
- [3]. M. S. Livingston, High-Energy Accelerators (Interscience Publishers Inc., New York, (1954).
- [4]. T. Beas, Nuclear Research Reactors in the World, (1999), <https://www.iaea.org/>
- [5]. J. Csikai, Handbook of Fast Neutron Generators, CRC Press, Inc., Boca Raton Florida, USA, (1987).
- [6]. Tak Pui Lou, Compact D-D/D-T Neutron Generators and Their Applications, 2003, A dissertation (thesis) in Engineering-nuclear engineering University of California, Berkeley.
- [7]. Hamid Aït Abderrahim, Didier De Bruyn, Gert Van den Eynde, Rafaël Fernandez, Accelerator Driven Subcritical Systems, Encyclopedia of Nuclear Energy, Elsevier, 2021, Pages 191-202, <https://doi.org/10.1016/B978-0-12-819725-7.00093-3>.
- [8]. Y. Saji, Journal of the Physical Society of Japan, 15(3) (1960) 367-371.
- [9]. J. W. Meadows, Nuclear Instruments and Methods in Physics Research A, 324 (1993) 239-46.
- [10]. NuDat 3.1, National Nuclear Data Center, Brookhaven National Laboratory, <https://www.nndc.bnl.gov/>
- [11]. P. Singh, Folded tandem ion accelerator facility at trombay, Pramana 57 (2001) 639-650.
- [12]. S. Santra, P. Singh, Beam optics of the folded tandem ion accelerator at BARC, Pramana 59 (2002) 53-68.
- [13]. S. Santra, K. Mahata, P. Singh, C. V. Fernandes, M. Hemalatha, S. Kailas, Beam energy calibration for the folded tandem ion accelerator, Nuclear Instruments and Methods in Physics Research A 496 (2003) 44-50.

- [14]. R. P. Sharma, 14 UD Pelletron accelerator project at TIFR, Nuclear Instruments and Methods in Physics Research Section A: Accelerators, Spectrometers, Detectors and Associated Equipment, Volume 244, Issues 1–2 (1986) 52-53.
- [15]. P. V. Bhagawat, Improvement in performance and operational experience of 14 UD Pelletron Accelerator Facility, BARC–TIFR, PRAMANA Journal of Physics 59 (5) (2002) 719-724.
- [16]. E. V. Sayre, Methods and applications of activation analysis, Ann. Rev. Nucl. Sci. 13 (1963) 145-162.
- [17]. R. C. Kotch, Activation Analysis Hand Book, Academic Press, New York and London (1960).
- [18]. Ian Rittersdorf, Gamma ray spectroscopy, Nuclear Engineering and Radiological Sciences (2007) retrieved from <http://www-personal.umich.edu/~ianrit/gammaspec.pdf>
- [19]. Gordon R. Gilmore, Practical Gamma-Ray Spectrometry, Book, 2008, John Wiley and Sons, Ltd, DOI: 10.1002/9780470861981, ONLINE ISBN: 9780470861981.
- [20]. Tim Vidmar, EFFTRAN-A Monte Carlo efficiency transfer code for gamma-ray spectrometry, Nuclear Instruments and Methods in Physics Research Section A: Accelerators, Spectrometers, Detectors and Associated Equipment Volume 550 (3) (2005) 603-608.